

Experimental and numerical investigation of the cylindrical blade tube inserts effect on the heat transfer enhancement in the horizontal pipe exchangers

Sendogan Karagoz¹ · Faraz Afshari¹ · Orhan Yildirim¹ · Omer Comakli¹

Received: 29 September 2016 / Accepted: 13 March 2017 / Published online: 22 March 2017
© Springer-Verlag Berlin Heidelberg 2017

Abstract In this experimental and numerical study an attempt to enhance the heat transfer rate by cylindrical blade that form turbulence flow inside the exchanger pipe is carried out. The effects of the blade geometry are also examined to investigate heat transfer rate in experimented tube inserts. Experiments are performed in different blade spacing ($Sy_{1,2,3} = 101\text{--}216\text{--}340$ mm) and various blade angles ($\alpha_{1,2,3} = 0^\circ\text{--}45^\circ\text{--}90^\circ$). The water flow rate inside the tube is adjusted in three different ranges to approach intended Reynolds numbers ($Re_{1,2,3} = 6000\text{--}11,000\text{--}17,000$). Nusselt number, Reynolds number and effect of friction factor are investigated separately. For all experiments, the increase in Nu number due to used tube inserts is recorded and compared to each other and plain tube in the related profiles. It is concluded that installed tube inserts in the heat exchanger tube, led to a significant increase in Nu number and energy saving. Among different experimented cases, using mean value in various Re numbers, the highest Nusselt number was obtained at $Sy_1 = 101$ mm which was 24% more than that of plain tube. This value was 18.7 and 8.3% for $Sy_2 = 216$ and $Sy_3 = 340$ mm respectively. By this way, according results for friction factor were 0.30, 0.19 and 0.14. The presented study has been simulated by

ANSYS Fluent 16 software to analyze flow behavior and heat transfer characteristics.

List of symbols

A	Pipe cross-sectional area (m^2)
A_t	Total surface area of pipe (m^2)
D	Pipe inside diameter (m)
f	Friction factor
g	Gravity (m/s^2)
h	Heat transfer coefficient ($W/m^2 K$)
S_y	The distance between two blades (m)
α	Blade angle
L	Length of the tube (m)
\dot{m}	Mass flow rate (kg/s)
Nu	Nusselt number
PEC	Performance evaluation criteria
P	Pressure (bar)
ΔP	Pressure drop (bar)
\dot{Q}	Heat transfer (kW)
R	Radius (m)
Re	Reynolds number
t	Time (s)
T	Temperature ($^\circ C$)
ΔT	Temperature difference ($^\circ C$)
ΔT_s	Wall temperature difference ($^\circ C$)
T_f	Fluid temperature ($^\circ C$)
U	Velocity (m/s)
V	Volume (m^3)
V'	Inner net volume of the tube (m^3)
\dot{V}	Volumetric flow (m^3/s)
Z	Distance between thermocouples (m)
μ	Dynamic viscosity (kg/ms)
v	Velocity (m/s)
ρ	Density (kg/m ³)
k	Thermal conductivity of fluid (W/m K)

✉ Sendogan Karagoz
skaragoz@atauni.edu.tr

Faraz Afshari
faraz.afshari@atauni.edu.tr

Orhan Yildirim
yildirimorhan.100@gmail.com

Omer Comakli
ocomakli@atauni.edu.tr

¹ Department of Mechanical Engineering, Atatürk University, 25240 Erzurum, Turkey

Subscripts

in	Inlet
out	Outlet
e	Effective
f	Friction
l	Liquid phase
w	Wall
s	Balancing tank
sis	System

1 Introduction

There are various heat transfer enhancers were presented in the literature include: porous material, vortex turbulators, fins, nanofluids, phase-change devices, high thermal conductivity composite materials, and large particle suspensions. Generally, the applied method to increase heat transfer is considered as heat transfer augmentation or enhancement. Recently, numerous thermal scientists and engineers are probing for new methods with high heat transfer augmentation between the fluid and surface. Basically, mechanisms of enhancing heat transfer have been classified as active or passive methods by Bergles. Active enhancement methods require external power such a vibrating the surface, fluid or well stirring.

However, the passive enhancement methods do not require external power to reinforce the enhancement characteristics. Some examples of passive methods are: extended surfaces, rough surfaces, coiled tubes, additives for fluids, swirl flow devices. Furthermore, the heat transfer approach can be improved via various mechanisms, including increasing the temperature difference between the fluid and the surface, increasing the fluid flow rate, enhancing effective thermal conductivity of solid and fluid under dynamic and static conditions, disruption of the laminar sublayer, promoting flow attachment, increasing the order of the fluid molecules and modification of radioactive property [1].

It can stated that, the most significant variables in reducing the cost and size of heat exchangers are the heat transfer coefficient and pressure drop. In the exchangers, some approach is needed to enhance the process of heat transfer and improving efficiency. Researchers have made excellent effort and used an effective technique to increase heat transfer rate by using tube inserts to produce swirl flow and reduce the thickness of the thermal boundary layer. However, it was realized that the flow resistance is also increased with this method. Hence, in order to evaluate the thermo-hydrodynamic performance of such techniques, performance evaluation criteria (PEC) were proposed which indicate that a larger heat transfer rate does not mean a better overall performance [2].

The effects of twin-counter/co-twisted tapes on friction factor, heat transfer rate, and thermal enhancement index were determined. The twin counter twisted tapes were utilized as counter-swirl flow generators while twin co-twisted tapes were used as co-swirl flow generators in a test section under uniform heat flux conditions for Reynolds numbers range between 3700 and 21,000. The study revealed that heat transfer rates in the tube fitted with the twin counter twisted tapes were around 12.5–44.5 and 17.8–50% higher than those with the twin co-twisted tapes and single twisted tapes, respectively [3]. Several longitudinal rectangular plate inserts applied as tube side heat transfer augmentative apparatus which have been numerically studied. The effects of the radius ratio of the circumscribed circle of the rectangular plate to the tube, the aspect ratio of the rectangular plate and the eccentric installation on the net effect between heat transfer augmentation and pressure drop have been determined [4]. The helical tapes inserted in a tube were investigated experimentally to generate swirl flow that helps to increase the heat transfer rate of the exchanger in a range of Reynolds number between 2300 and 8800. The regularly spaced helical tape inserts at s (space to tape ratio) = 0.5 yields the maximum Nusselt number which was around 50% above the plain tube [5]. Double pipe heat exchanger fitted with regularly spaced twisted tape elements, were studied to find out heat transfer rate and friction factor characteristics experimentally. In shell side and tube side, cold and hot water were used as working fluids [6].

Three kinds of tube inserts, including longitudinal strip inserts (both with and without holes) and twisted-tape inserts with three different twisted angles were investigated for different inlet frontal velocity. Numerical simulation was performed by a 3D turbulence analysis of the heat transfer and fluid flow. It was determined that the heat transfer coefficient and the pressure drop with the longitudinal strip inserts were 7–16 and 100–170% higher than those of plain tubes without inserts [7]. Guo et al. proposed a center-cleared twisted tape aiming at achieving good thermo hydraulic performance. The study was performed numerically in laminar flows. It was presented that the center-cleared twisted tape is a capable technique for heat transfer enhancement. The thermal performance factor with center-cleared twisted tape can be enhanced by 7–20% in comparison to the tube with conventional twisted tape [8]. Sivashanmugam et al. studied friction factor and heat transfer of circular tube fitted with full-length helical screw element of different twist ratio with uniform heat flux experimentally. It was observed that the heat transfer coefficient increases with twist ratio [9].

The coiled wire is one of the common heat transfer enhancement devices. These turbulators generate almost-periodic vortices into the flow while increasing the heat

transfer rate. In another investigation, the properties of these vortices, flow-acoustic coupling and the relation between vortex characteristics and entropy generation were studied experimentally [10]. The pressure drop in the horizontal double pipes and heat transfer enhancement with twisted tape with different relative pitches insert were investigated and the obtained results were compared with those without twisted tape [11]. In a study experimental measuring of the axial heat transfer distributions and the pressure drop coefficients of the tube fitted with a broken twisted tape was tested in the Reynolds range of 1000–40,000. Heat transfer coefficients, mean Fanning friction factors and thermal performance factors using the broken twisted tape were augmented to 1.28–2.4, 2–4.7 and 0.99–1.8 times of those in the tube fitted with the smooth twisted tape [12]. Flow-induced vibration of conical-ring turbulators used for enhancing the heat transfer rate. The conical-rings, having various pitches, were inserted into a pipe-line through which air was passed as the working fluid. Yakut et al. [13] showed that the Nusselt number increases with the increasing Reynolds number and the maximum heat transfer is obtained for the smallest pitch in the experiments. Influences of V-nozzle turbulator inserts in conjunction with a snail entry on heat transfer and friction loss characteristics in a circular tube were experimentally investigated. Converging–diverging nozzles like a venturi structure were used as a turbulator/reverse-flow generator which were placed inside the test tube where the air was selected as the test fluid. Heat transfer rate in the tube was examined in the Reynolds number ranging from 8000 to 18,000 [14].

The heat transfer enhancement in a tube with the circular cross sectional rings was investigated. Inserted rings near the tube wall were analyzed in different spacing. Uniform heat flux was applied to the external surface of the tube and the air was applied as working fluid in the range of Reynolds number 4475–43,725. The results for Nusselt number, friction factor and enhancement ratios for the tube with rings were presented [15]. In the electronic equipment the heat sinks are commonly installed in the restricted space of the systems and their thermal performance can be improved both by enhancing the heat transfer rate and by reducing the friction factor. In a study, the thermal performance characteristics of “S-shaped” elements were investigated in the wide range of Reynolds number to reveal the Nusselt number and friction factor [16]. Exergy analysis have been also done for the different type of turbulators including conical spring turbulators [17].

A plain tube and tube equipped with the three types of internal grooves (circular, square and trapezoidal) were studied in the computational fluid dynamics area to find out heat transfer, pressure drop, friction factor, Nusselt number and thermal hydraulic performance of the exchanger [18]. A number of investigations were carried out to show the effect

of the jagged insert on the efficiency and Nusselt number. Experimental and CFD investigations on the Nusselt number, friction factor and thermal–hydraulic performance of a tube using the classic and three modified twisted tape inserts were done. Obtained Nusselt number and performance of the jagged insert were greater than other types. The highest increase of 31 and 22% were observed in the Nusselt and performance of the jagged insert as compared with the classic types [19].

In this study, the innovative type of cylindrical blade tube inserts has been considered to investigate their effects on the vortices formation and consequently the efficiency of suggested turbulators in the heat transfer enhancement. In the experiments, various cylindrical blade turbulators (with different angles and spacing) are presented in order to enhance heat transfer rate in a circular tube and also different designed turbulators are compared to each other and analyzed by numerical simulation in a CFD program (ANSYS-Fluent [22]).

2 Experimental setup and test procedure

In the experiments, the plain tube made of Cr–Ni (stainless steel-316 L) has an inner diameter (d) of 13.5 mm, wall thickness of 2 mm and length (L) of 1020 mm. Different test samples are defined for various tube inserts with different angles (0° – 45° – 90°) and different blade spacing (101–216–340 mm) which are tested in the three different Reynolds numbers including 6000, 11,000 and 17,000 as shown in the test plan at Table 1.

The Reynolds number is an essential dimensionless quantity that is widely used in the science and technology, including exchangers to predict the flow patterns and heat transfer characteristics in different fluid flow situations. On the other hand, in the heat transfer from a boundary to a fluid, the Nusselt number can be defined as the ratio of convective heat transfer to that of conductive along the boundary. It can be stated that, the conductive term can be measured as the heat convection but with a motionless fluid. Basically, In the forced convection (like presented study), the Nu number is originally a function of the Re and Pr (Prandtl) number and selected range of Reynolds is a significant key in experiments to reveal the flow patterns and heat transfer enhancement under different flow situations. Considering early researches in this field of science, selected Re numbers are mostly in the range of 2000 to 20,000 [3, 5, 6, 9, 14] so in this study selected Re numbers are 6000, 11,000 and 17,000.

In the experiments, the cold water flow rate is adjusted by a manual valve to approach the intended Reynolds number. Details of experimental setup in the laboratory and a schematic diagram of whole installed system are presented respectively in Figs. 1 and 2, while the details of geometry characteristics of tube insert turbulators are shown in Figs. 3 and 4.

Table 1 Test plan

Samples	No.	S_y (mm)	α (°)	Re
A (10 blades—0°)	1	101	0	6000
	2	101	0	11,000
	3	101	0	17,000
B (10 blades—45°)	4	101	45	6000
	5	101	45	11,000
	6	101	45	17,000
C (10 blades—90°)	7	101	90	6000
	8	101	90	11,000
	9	101	90	17,000
D (5 blades—45°)	10	216	45	6000
	11	216	45	11,000
	12	216	45	17,000
E (5 blades—0°)	13	216	0	6000
	14	216	0	11,000
	15	216	0	17,000
F (5 blades—90°)	16	216	90	6000
	17	216	90	11,000
	18	216 </td <td>90</td> <td>17,000</td>	90	17,000
G (3 blades—90°)	19	340	90	6000
	20	340	90	11,000
	21	340	90	17,000
H (3 blades—45°)	22	340	45	6000
	23	340	45	11,000
	24	340	45	17,000
I (3 blades—0°)	25	340	0	6000
	26	340	0	11,000
	27	340	0	17,000

Initially, selected cylindrical blades are inserted in the tube along the test section to produce turbulent flow. The tube is heated by electrical wire around to provide a uniform heat flux condition. The DC electrical heat power is applied and also controlled by a variac transformer to provide a constant heat rate of 1100 W along the entire length of the test tube. The outer surface of the test tube has been insulated to prevent convective heat leak to ambient. The inlet and outlet temperatures of the fluid (water) are measured with two T type thermocouples. For this reason, 5 mm diameter end closed copper tubes submerged inside the main tube with their thermocouples have been used and also several thermocouples installed on the wall around the core tube have been used to measure the outer surface temperatures that determine mean temperature of the wall. As shown in Fig. 5, wall temperatures have been measured with 11 thermocouples along the top of the wall and also 11 thermocouples along the bottom of the wall in equal intervals (totally, 24 T type thermocouples have been used). The test loop consists of a balancing tank of 0.0075 m³ to keep the pressure of the system in the expected range, a water pump for circulation (centrifugal type pump-maximum working pressure: 6 bar, flange: DN40–DN100), Bourdon type Manometers in the inlet and outlet of the test tube, electromagnetic flowmeter (Euromag), data logger (data transferred to PC by Advantech PC-LabCard), T type thermocouples, and heat exchanger to prepare required fluid temperature and heat transfer test section. For all experiments, it is necessary to get results and record all data including temperature, pressure drop of the test fluid (water) and volumetric flow rate at steady state conditions while the temperature of inlet water is maintained constant.

**Fig. 1** A picture of experimental setup

3 Uncertainty analysis

Experimental uncertainties can result from instrument selection, calibration, observation, reading, planning, and some of them are environmental errors. In our experimental study, uncertainty for temperatures measured by T type copper-constantan thermocouples $\pm 0.5\%$, pressures by Bourdon-type manometers $\pm 0.08\%$, electrical power $\pm 0.4\%$, and uncertainty for water flow rate is $\pm 1.60\%$. The total uncertainty of calculated Nusselt number and friction factor can be obtained by the following equations, from which by using the Kline and McClintock method calculated uncertainty for Nusselt and friction factor are ± 2.8 and $\pm 2.3\%$ respectively [20].

$$Un_{Nu} = \sqrt{\left(U_{\dot{Q}} \frac{\partial Nu}{\partial \dot{Q}}\right)^2 + \left(U_{T_w} \frac{\partial Nu}{\partial T_w}\right)^2 + \left(U_{T_{in}} \frac{\partial Nu}{\partial T_{in}}\right)^2 + \left(U_{T_{out}} \frac{\partial Nu}{\partial T_{out}}\right)^2} \quad (1)$$

Fig. 2 Schematic diagram of experimental setup

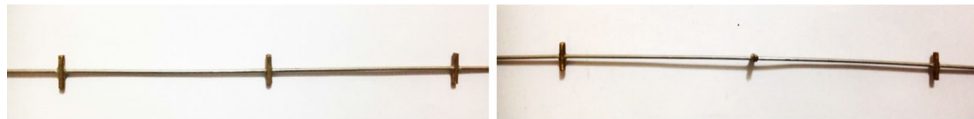
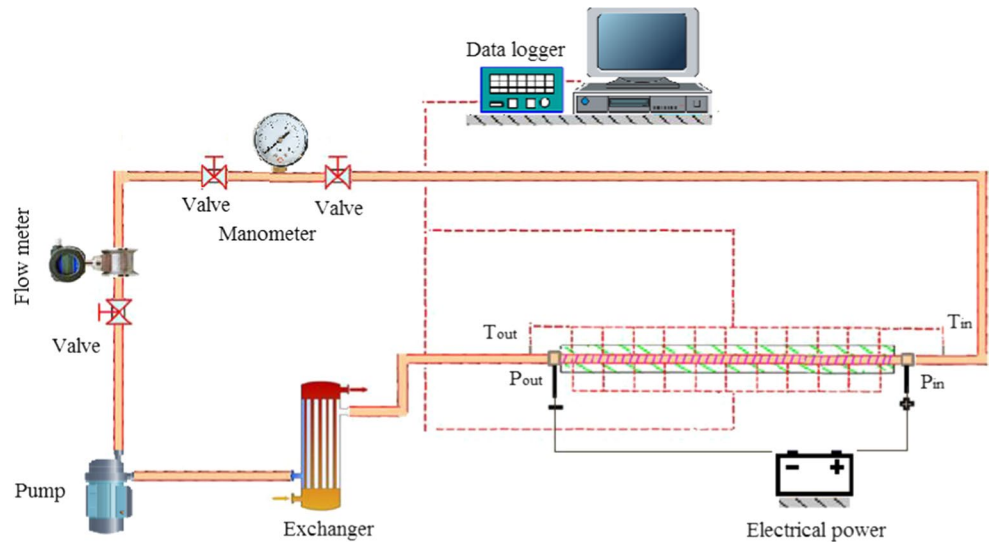


Fig. 3 Pictures of tube inserts in 0° (left) and 90° (right) blade angle

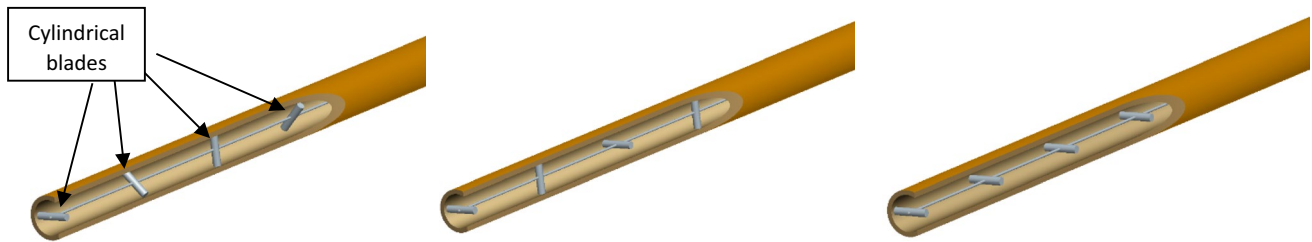


Fig. 4 Schematic image of tube insert geometries in various blade angle

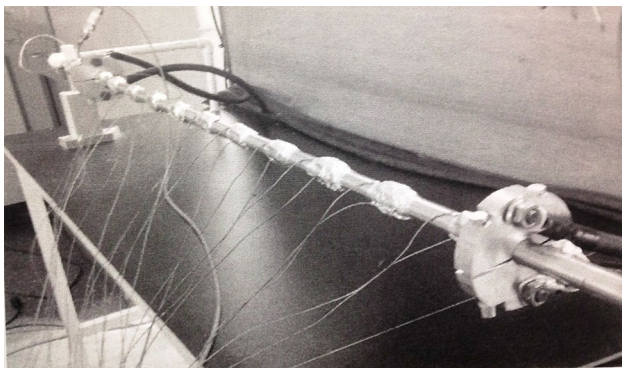


Fig. 5 Schematic view of test tube with measuring devices

$$U_{nf} = \sqrt{\left(U_{Pin} \frac{\partial f}{\partial Pin} \right)^2 + \left(U_{Pout} \frac{\partial f}{\partial Pout} \right)^2 + \left(U_v \frac{\partial f}{\partial v} \right)^2} \quad (2)$$

4 Calculation

During the experiments, the heat transfer rate is assumed to be in a steady state condition. Moreover, according to a research carried out by Hsieh et al. [21] radiation heat loss is approximately 3% of the input power and also considering the fact that the test section is well insulated, heat transfer is equal to the heat loss from the test section by cooling water in the tube. Electrical power energy provided for heat transfer can be also stated as,

$$\dot{Q} = VI = \dot{m}_w c_p (T_{out} - T_{in}) \tag{3}$$

The heat transfer coefficient in the tube wall due to convection can be written as,

$$h = \frac{\dot{Q}}{A \left[T_w - \left(\frac{T_{in} + T_{out}}{2} \right) \right]} \tag{4}$$

where T_{out} and T_{in} are the outlet and inlet water temperature, T_w is the mean temperature of the tube wall and A is the inside surface area of the tube and can be expressed as:

$$A = \pi DL \tag{5}$$

In the experimental results, the average Nusselt number can be calculated as,

$$Nu = \frac{hD}{k} \tag{6}$$

The fluid local thermal conductivity (k) is obtained from the fluid properties at the local mean bulk fluid temperature [$T_b = (T_{out} + T_{in})/2$].

Using pressure loss, ΔP , the tube friction factor can be computed across the test length, by following equation:

$$f = \frac{\Delta P}{(L/D)(\rho v^2/2)} \tag{7}$$

The Reynolds number based on the total flow rate at the inlet section is expressed as:

$$Re = \frac{\rho v d_e}{\mu} \tag{8}$$

where μ is the dynamic viscosity of the working fluid, v is the average velocity and effective diameter (d_e) for tube insert can be written as the following equation: (in the case of plain tube d_e is equal to inner diameter)

$$d_e = \sqrt{\frac{4V'}{\pi L}} \tag{9}$$

V' is the net volume of the test section and can be calculated by total inside volume and tube insert volume as,

$$(V' = V_{tube} - V_{turbulator}) \tag{10}$$

For validation test results, the obtained values for Nusselt number (Nu) and friction factor (f) of the plain tube are evaluated by comparing the previous correlations under similar conditions.

For the plain tube, the empirical correlations of the Nusselt number can be stated as [5],

$$Nu = 0.023 Re^{0.8} Pr^{1/3} \text{ Colburn correlation (for } 10^4 \leq Re) \tag{11}$$

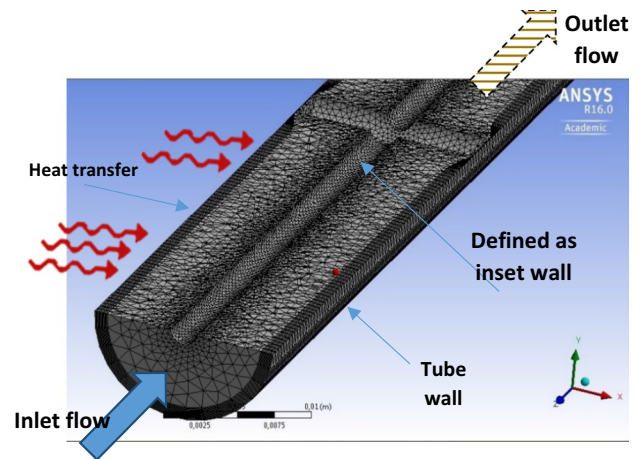


Fig. 6 A schematic view of the mesh quality and boundary condition

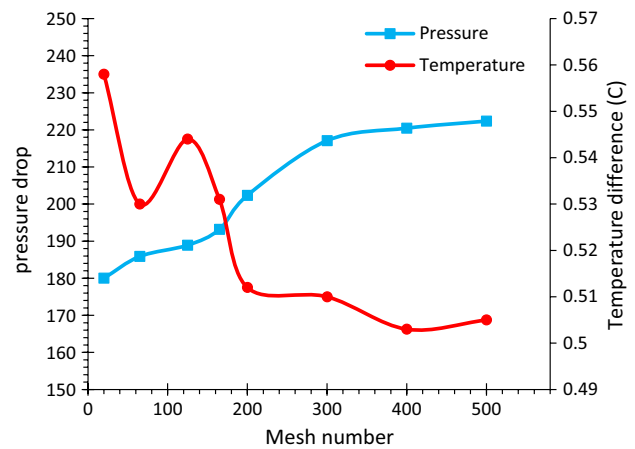


Fig. 7 Mesh analysis with obtained data from pressure and temperature differences

$$Nu = 0.023 Re^{0.8} Pr^n \text{ (n = 0.3–0.4) Dittus-Boelter correlation (for } 10^4 \leq Re) \tag{12}$$

$$Nu = \frac{\left(\frac{f}{8}\right)(Re \cdot Pr)}{1.07 + 12.7 \left(\frac{f}{8}\right)^{1/2} \left[Pr^{2/3} - 1\right]} \text{ Petukhov correlation (for } 3000 \leq Re \leq 5 \times 10^6) \tag{13}$$

On the other hand, friction factor values for plain tube are also computed with Eqs. (14, 15) which are proposed in the literature [10] as,

$$f = 0.316 Re^{-0.25} \text{ Blasius correlation (Re } \leq 20,000) \tag{14}$$

$$f = (0.790 \ln Re - 1.64)^{-2} \text{ Petukhov correlation (for } 3000 \leq Re \leq 5 \times 10^6) \tag{15}$$

Fig. 8 Residual variations versus iteration number

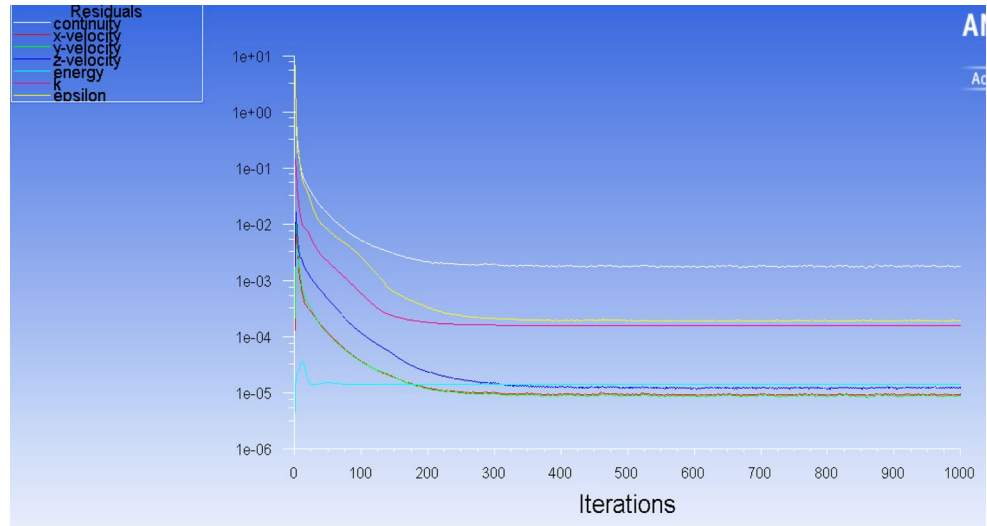


Table 2 Uncertainty and convergence criteria of the numerical solution

Iteration	Continuity	x-velocity	y-velocity	z-velocity	Energy	k	ϵ
1000	$<4.1 \times 10^{-4}$	$<1.8 \times 10^{-6}$	$<1.6 \times 10^{-6}$	$<4.4 \times 10^{-6}$	$<7 \times 10^{-6}$	$<5.7 \times 10^{-5}$	$<5.3 \times 10^{-5}$

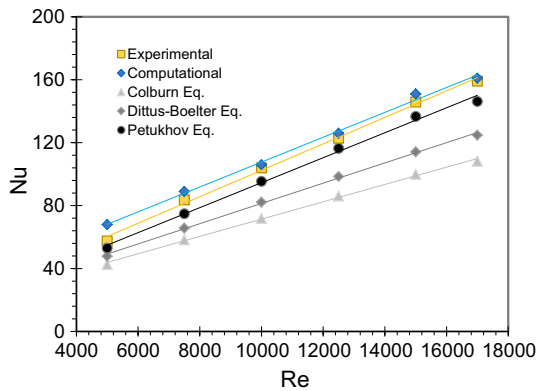


Fig. 9 Computed and experimental results of Nusselt number versus Re for plain tube

In the heat transfer enhancement techniques, enough attention should be paid to friction factor value, flow resistance increase and performance factor of the presented methods. In order to evaluate the performance of the experimented tube inserts, overall thermo-hydrodynamic performance can be calculated by “performance evaluation criteria” (PEC) [2],

$$PEC = \frac{Nu/Nu_0}{\left(\frac{f}{f_0}\right)^{1/3}} \quad (16)$$

where Nu_0 and f_0 are the Nusselt number and friction factor of the plain tube,

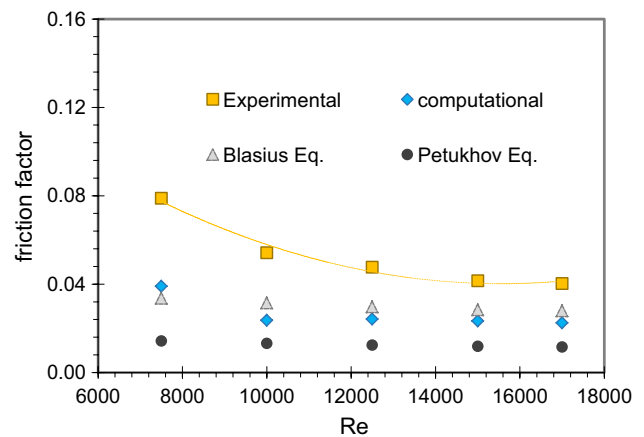


Fig. 10 Friction factor by equations, experimental and computational methods versus Re for plain tube

4.1 CFD analysis

ANSYS Fluent 16 program is used to solve the defined problem that can be assumed to be three dimensional with turbulent flow. Figure 4 shows a schematic view of geometry where the analysis domain has been defined and various simulations performed numerically in this region. Different spacing between the cylindrical blades and their angles are considered as mentioned in the test procedure section. At this stage, the following assumptions for fluid

are applied in the derivation of continuity, momentum and energy equations,

- fluid is incompressible,
- the physical properties of fluid are constant,
- the effect of gravity is negligible.

Basically, conservation equations can be expressed as:

Mass conservation:

$$\frac{\partial \rho}{\partial t} + \frac{\partial}{\partial x_i}(\rho v_i) = 0 \tag{17}$$

Momentum equation:

$$\frac{\partial}{\partial x_j}(\rho v_i v_j) = \frac{-\partial P}{\partial x_i} + \frac{\partial}{\partial x_j} \left[\mu \left(\frac{\partial v_i}{\partial x_j} + \frac{\partial v_j}{\partial x_i} \right) - \frac{2}{3} \mu \frac{\partial v_k}{\partial x_k} \delta_{ij} \right] \tag{18}$$

Energy conservation:

$$\begin{aligned} \frac{\partial}{\partial t}(\rho e) + \frac{\partial}{\partial x_j} \left(\rho v_j c_p T - k \frac{\partial T}{\partial x_j} \right) &= u_j \frac{\partial p}{\partial x_j} \\ + \left[\mu \left(\left(\frac{\partial v_i}{\partial x_j} + \frac{\partial v_j}{\partial x_i} \right) - \frac{2}{3} \frac{\partial v_k}{\partial x_k} \delta_{ij} \right) \right] \end{aligned} \tag{19}$$

In the present problem, $k - \epsilon$ RNG model with enhanced wall functions for the near wall treatment is used in the CFD program as follows:

$$\begin{aligned} \frac{\partial}{\partial t}(\rho k) + \frac{\partial}{\partial x_i}(\rho k v_i) \\ = \frac{\partial}{\partial x_j} \left[\left(\frac{\mu + \mu_t}{\sigma_k} \right) \frac{\partial k}{\partial x_j} \right] \\ + \mu_t \left(\frac{\partial v_i}{\partial x_j} + \frac{\partial v_j}{\partial x_i} \right) \frac{\partial v_i}{\partial x_j} - \rho \epsilon \end{aligned} \tag{20}$$

$$\begin{aligned} \frac{\partial}{\partial t}(\rho \epsilon) + \frac{\partial}{\partial x_i}(\rho \epsilon v_i) \\ = \frac{\partial}{\partial x_j} \left[\left(\frac{\mu + \mu_t}{\sigma_\epsilon} \right) \frac{\partial \epsilon}{\partial x_j} \right] \\ + C_{1\epsilon} \frac{\epsilon}{k} \mu_t \left(\frac{\partial v_i}{\partial x_j} + \frac{\partial v_j}{\partial x_i} \right) \frac{\partial v_i}{\partial x_j} \\ - C_{2\epsilon} \rho \frac{\epsilon^2}{k} - \alpha \rho \frac{\epsilon^2}{k} \end{aligned} \tag{21}$$

$$\mu_t = \rho C_\mu \frac{k^2}{\epsilon} \tag{22}$$

In the present study, grid independence analysis has been done for the region between two blades and obtained data showed that the problem is converged in 400,000 cells. However, geometry has been meshed with maximum cell number (500,000 cells). The grid is well concentrated close to the wall and blades to get better results in the boundary conditions. Various cell types and sizes were examined and no considerable change was seen in finer cells. For mesh type, curvature mode and triangle surface were applied with volume statistics of 1.5×10^{-13} and 5.89×10^{-10} for minimum and maximum mesh size respectively. A view of the mesh configuration has been shown in Fig. 6.

Due to the pressure gradient, boundary layers, especially in regions close to the wall of the tube and inserts were meshed into small cells to obtain precise results. The second order upwind discretization scheme for energy, momentum, dissipation energy and turbulent kinetic energy, the SIMPLE pressure–velocity coupling algorithm, the standard pressure, were applied in the model.

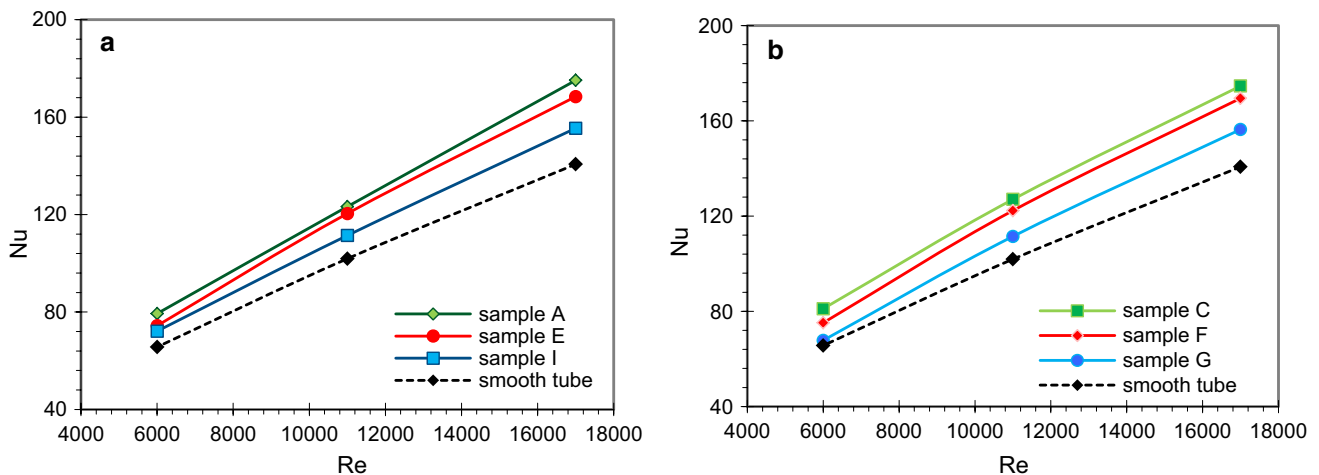


Fig. 11 a Experimental results of Nusselt number for samples A, E and I with $\alpha = 0^\circ$, b also samples C, F and G with $\alpha = 90^\circ$

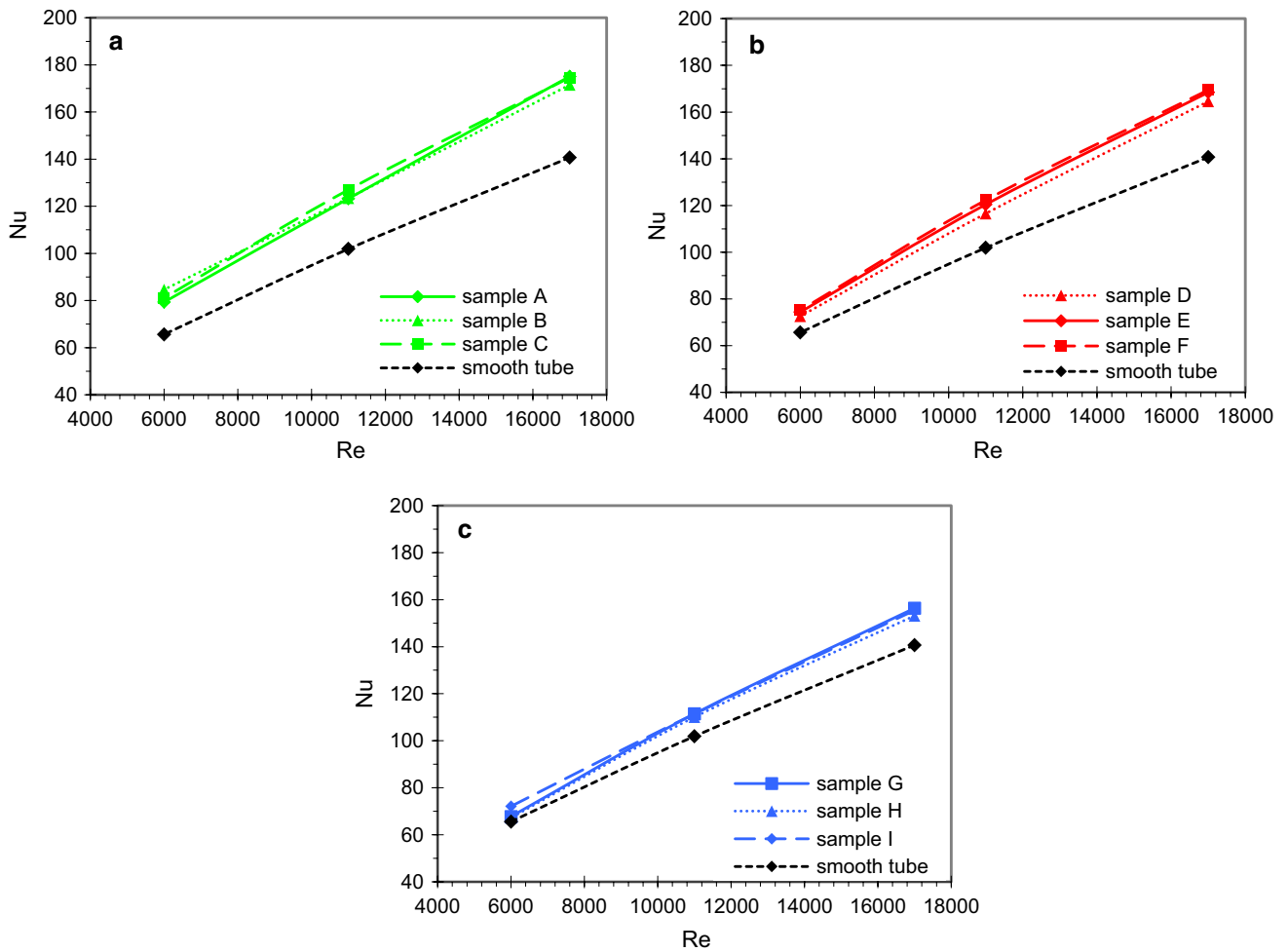


Fig. 12 Nusselt–Reynolds diagrams for various blade angles but same spacing, **a** blade distance of 101 mm, **b** blade distance of 216 mm, **c** blade distance of 340 mm

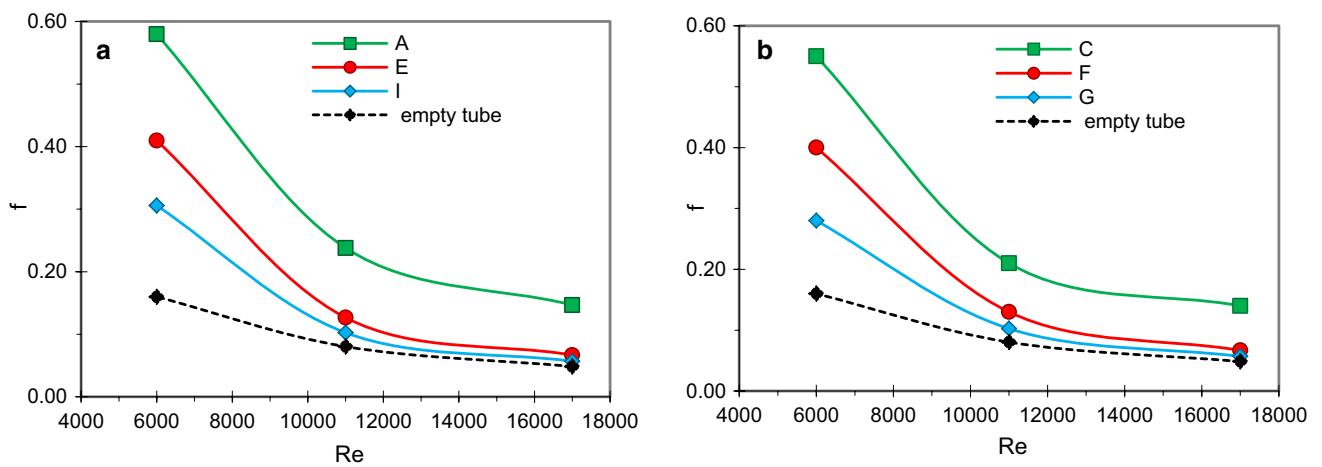


Fig. 13 **a** Experimental results of friction factor for samples A, E and I with $\alpha = 0^\circ$, **b** also samples C, F and G with $\alpha = 90^\circ$

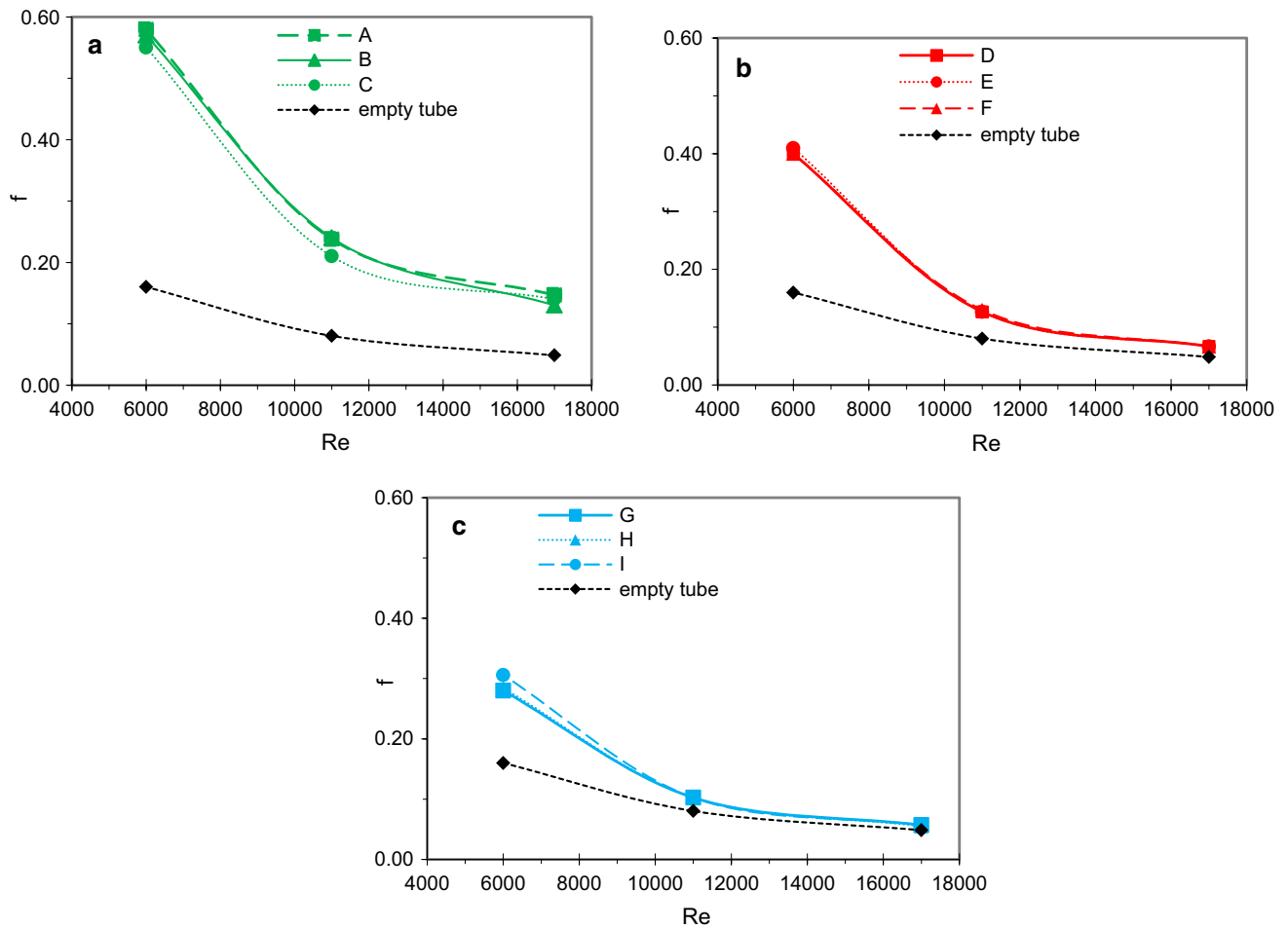


Fig. 14 Friction factor diagrams for various blade angles but same spacing, **a** blade distance of 101 mm, **b** blade distance of 216 mm, **c** blade distance of 340 mm

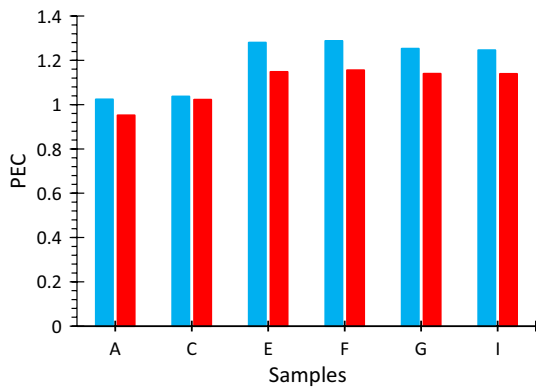


Fig. 15 Variation of the performance evaluation criteria (PEC) for different test samples in Reynolds number of 17,000 (*longer lines*) and 11,000 (*shorter lines*)

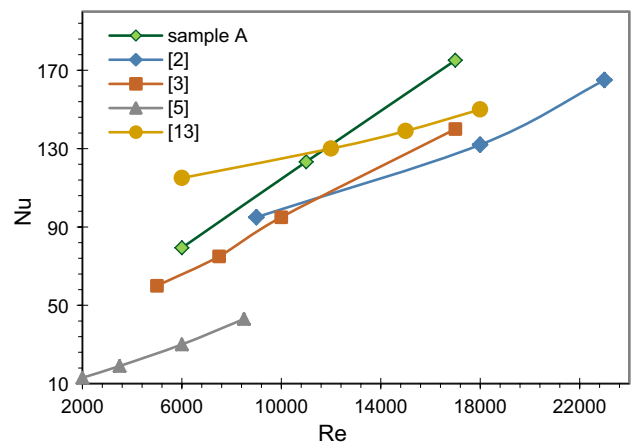


Fig. 16 Comparison between earlier studies with the obtained results from sample A. Ref. [2]: slant angle $\alpha = 10^\circ$, pitch 30 mm—Ref. [3]: single twisted tape—Ref. [5]: full-length helical with rod—Ref. [13]: conical ring

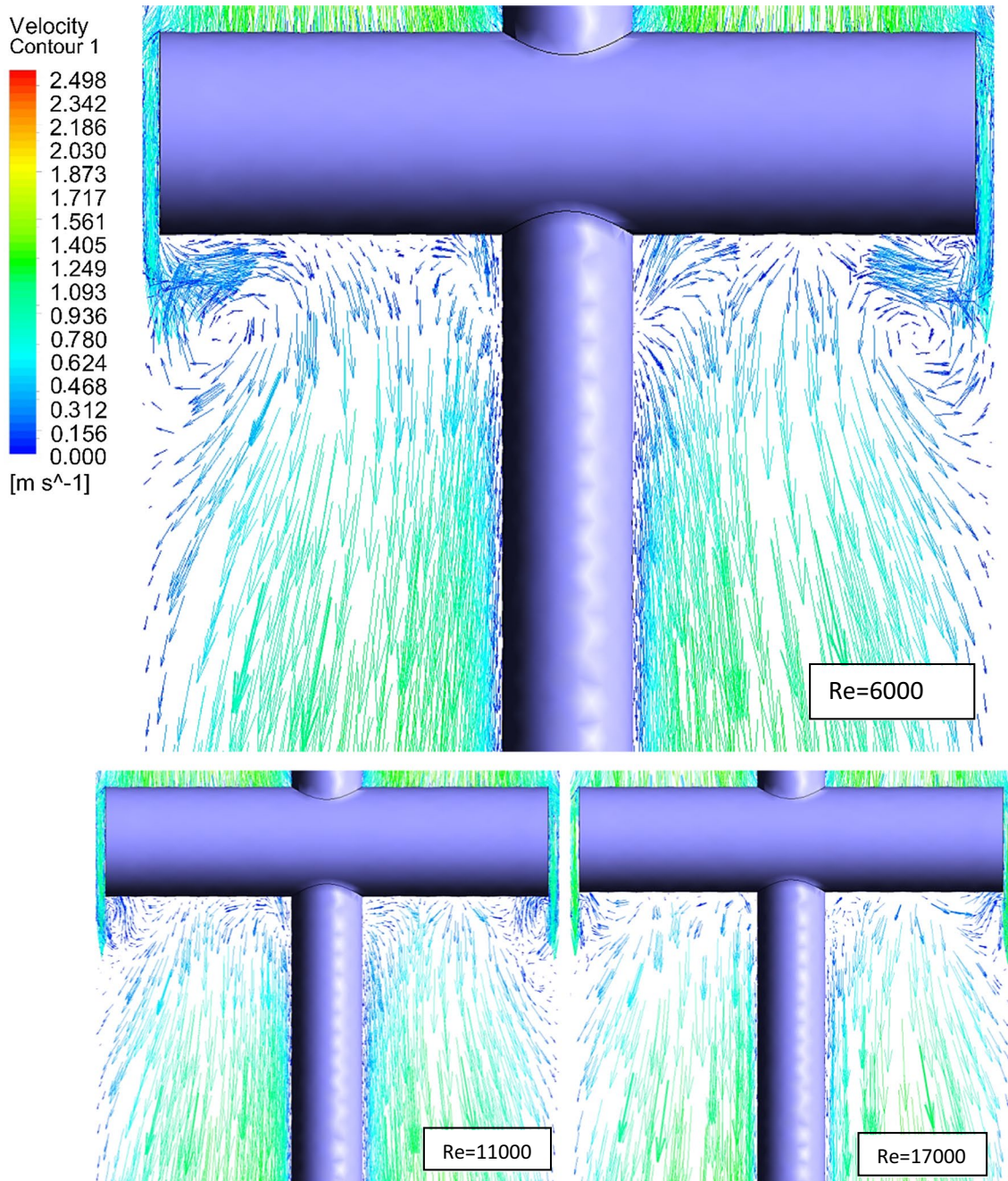


Fig. 17 Velocity vectors in front of the blade for different Re numbers (fluid flows up to down)

A number of techniques and methods are available to evaluate numerical uncertainties in the computational fluid dynamics. The significant criteria have been noticed in the computational analyzing as follows [23],

1. For acceptable results, numerical methods were selected second order (based on Taylor series expansion).
2. A range of various grid resolutions were tested (Fig. 7) to obtain grid-independence state.
3. Iterative convergence was precisely addressed and corresponding convergence was evaluated at 1000 iterations (Fig. 8).
4. The boundary conditions were precisely considered in terms of introduction, grids, solution method, etc. to minimize uncertainties (Fig. 6).

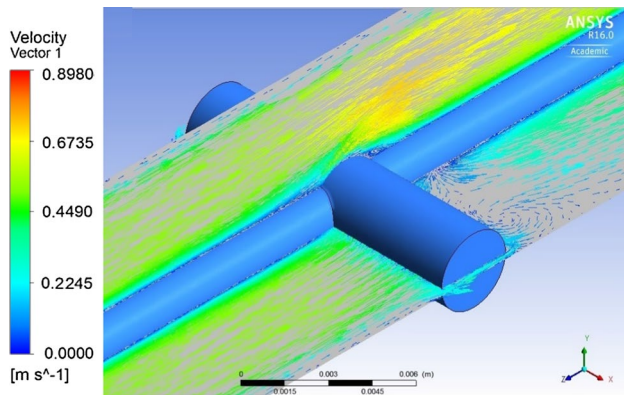


Fig. 18 3D velocity vectors around a blade at Re number of 6000

- Comparison with reliable experimental results, reasonable agreement with experimental data and appropriate analytical solutions were used to show accuracy for presented solution (Fig. 16–Eqs. 11, 12, 13).

Table 2 has been presented to show the accuracy of the calculation in the terms of convergence criteria and also mesh analysis has been provided in the Fig. 7 showing mesh quality by using obtained data from pressure and temperature differences. Convergence criteria has been identified in Fig. 8 to show the problem solving process in 1000 iteration. In this figure, variations of the continuity, velocity, energy, k and epsilon residuals has been presented respectively.

5 Results and discussion

Results of the study and obtained values of Nusselt number and friction factor are presented and discussed in this section. The outcomes from correlations and both

experimental and computational results in various Reynolds numbers have been gathered in the following figures. By referring to Fig. 9, it can be observed that in case of plain tube, as Re value increases Nu number increases. The increase in Nusselt represents an augmentation in heat transfer due to increase of convection.

In addition, variation of friction factor with Re number for the blank test tube is shown in Fig. 10. In this figure, experimental and CFD (computational) results are compared to the calculated results by Blasius and Petukhov equations (In the below figure, because of uncertainty in water flowmeter at low flow rate, the experimental results have little separated from the other calculated data at low Reynolds numbers).

The results on the figures reveal a good agreement with the former studies for both the Nusselt number (Nu) and the friction factor (f) correlations.

The provided results of heat transfer enhancement for the tubes fitted with different tube insert turbulators are also presented. Results are plotted for different blade spacing with $\alpha = 0^\circ$ and $\alpha = 90^\circ$ in Fig. 11a, b respectively. Tube inserts characteristic has been named in the previous section at Table 1 and are used in the following figures. In the given figures, it can be observed that Nusselt number increases with increases of Reynolds number. The overall obtained results indicate that in all cases where the tube is equipped with any type of tube inserts, the Nusselt number is higher than those without tube inserts. Moreover, the results display that the obtained Nusselt numbers for the tube insert with 10 blades are higher than others at all Reynolds numbers, which means, a further increase in the heat transfer rate as well as the temperature gradient near the wall.

Experiments for angle variations have been carried out for several times and it was determined that angle change in the turbulators has no substantial effect on the heat transfer. Figure 12 shows that Nusselt–Reynolds profiles are very close to each other and approximately identical in value. Hence, it can be concluded that, because of the

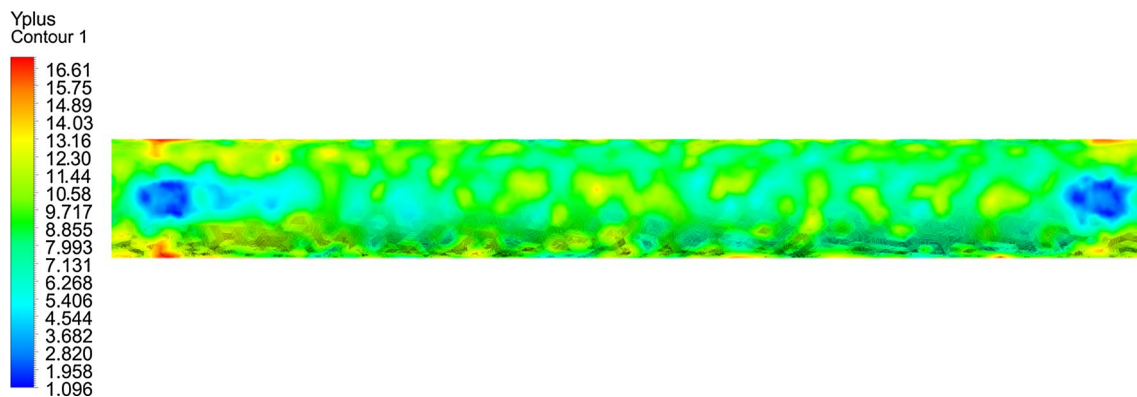


Fig. 19 Wall Y^+ contour for tube surface between two blades

simple production process and low cost, blades with 0° angle are preferred among the tested tube inserts for heat transfer enhancement.

Friction factor results have been analyzed for tube inserts as well as Nusselt numbers in all performed cases. Friction factor results have been provided for $\alpha = 0^\circ$ and $\alpha = 90^\circ$ in different blade spacing as shown in Fig. 13a, b. In the plotted diagrams, it can be observed that the pressure loss due to the presence of turbulator increases with the number of the blades. In other words, tube inserts with 10 blades have highest friction factor values and other types of tube inserts with 5 and 3 blades have placed in lower levels respectively. The effect of the various angles of turbulators have been compared in Fig. 14. Negligible changes in the friction factor results due to changes in the angle of cylindrical blades have been recorded which shows that blade angles have no major effect on the friction factor values.

The performance of the different test samples (PEC value) has been evaluated versus the Reynolds number of 17,000 and 11,000 in the Fig. 15. From the figure it is seen that the 5 blades tube inserts (sample E and F) have highest PEC value among the test samples. Finally, in this section some of previous works (references 2, 3, 5 and 13) have been selected and compared to the present study in the following diagram (Fig. 16),

6 Numerical analyses

3D numerical simulations for nine types of tube inserts, are performed at different fluid velocity for three corresponding Re number include 6000, 11,000 and 17,000. The numerical results have been provided to show the flow resistance and heat transfer rate on the parameters combination of the tube inserts. Basically, the convective heat transfer, boundary layer disturbing and fluid mixing have close relation to the geometry of the tube inserts. Hence, we introduce three-dimensional velocity vectors in front of the blade in different Re as an example to show the geometry impact, as presented in Figs. 17 and 18.

The wall Y^+ is a non-dimensional number is often calculated in CFD to describe how coarse or fine a mesh is for a particular flow. The wall Y^+ contour has been provided for tube surface between two blades in Fig. 19.

It is shown in Fig. 17 that the vortex in front of the blade becomes negligible when Re number increases from 6000 to 11,000 and 17,000. The boundary disturbing and mixing of the fluid are significantly augmented when the cylindrical blades are close to each other which causes to create thinner boundary layers and will result a notable increase in the friction factor. Due to the positive influence of boundary disturbing and fluid mixing at small S_y , the temperature gradient becomes larger in the boundary

layer simultaneously. Thus, outlet temperature shows a further increase because of enhanced heat transfer. To demonstrate the differences among the tube inserts with various blade angles we have solved the geometries for given Re numbers to investigate the velocity contours between two blades which are presented in Fig. 20.

It can be seen that how Re and blade angle effect on the velocity profile and fluid flow around the various tube inserts. In the low Re, less tangential velocity near the wall, means a much weaker fluid mixing and disturbance of the boundary layer. In front velocity fields of the tube insert with $\alpha = 45^\circ$ have been shown for given Re numbers in Fig. 21.

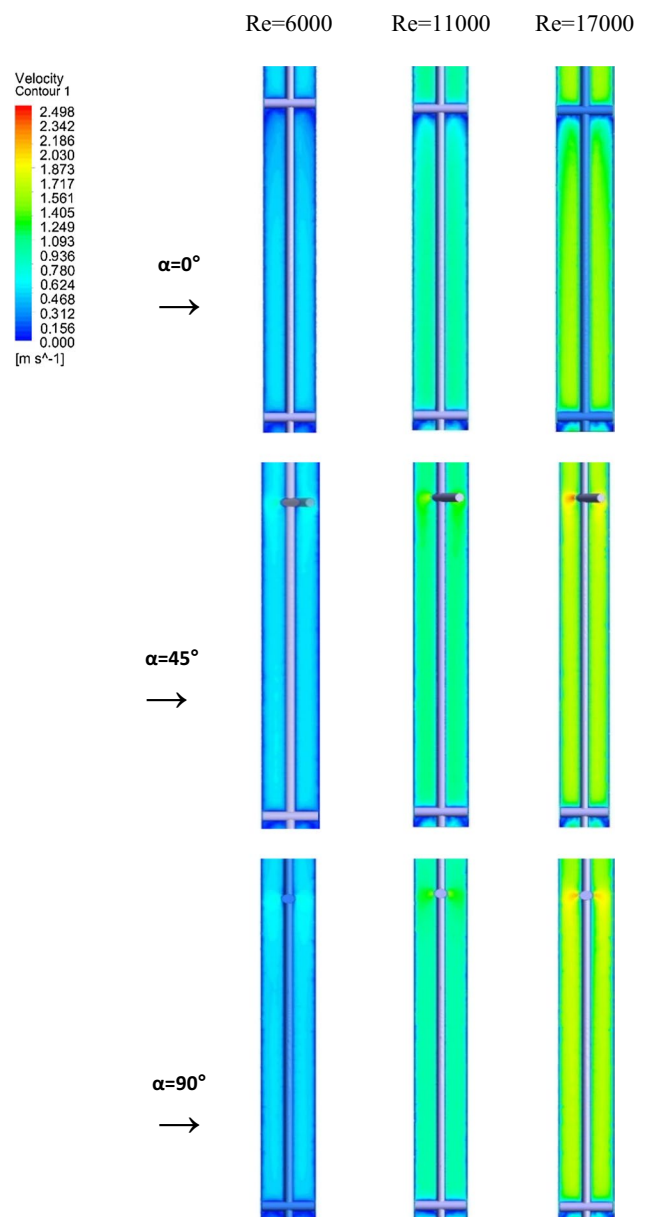


Fig. 20 Velocity contours for different Reynolds numbers with various angles

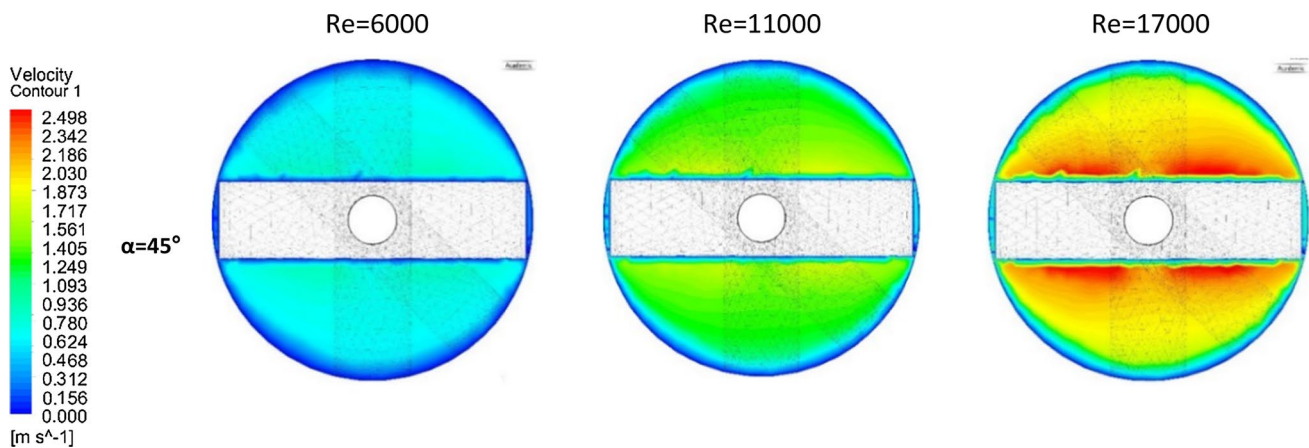


Fig. 21 In front velocity contours for three different Reynolds numbers with angle of 45°

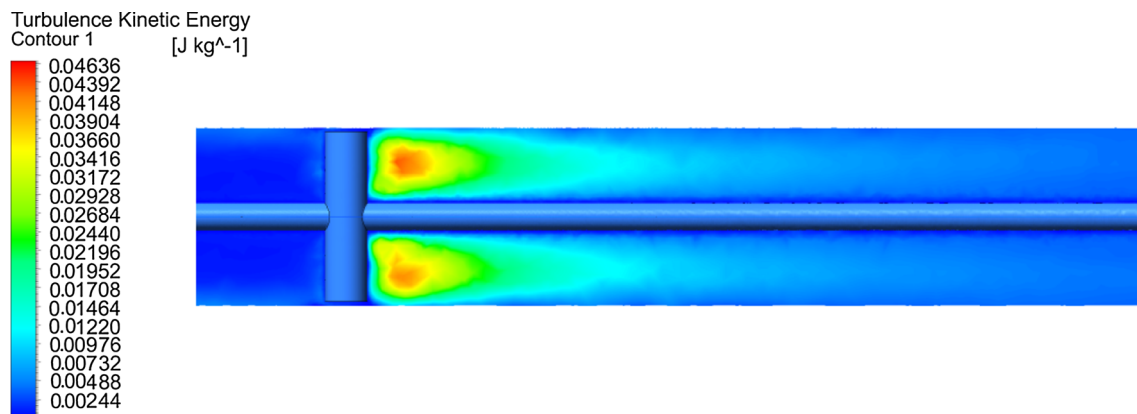


Fig. 22 Turbulence kinetic energy contour at Re number of 6000 (flow direction is from *left to right*)

The effect of the tube insert on the turbulence kinetic energy is presented at Fig. 22 and also the temperature fields for same distance blades shown in Fig. 23 demonstrate that, the thermal boundary layers grow as the Re number and blades angle change in different geometry of the tube insert turbulators. In other words, in high Re and well disturbed flow, temperature gradient near the wall gets smaller. All of these cases confirm that the boundary layer disturbance and mixing fluid are the key factor in the heat transfer enhancement.

7 Conclusion

In this experimental and numerical study, tube inserts used to achieve turbulent flow for heat transfer augmentation. Three different blade spacing, three different blade angle and three different ranges of Reynolds number were performed to analysis heat transfer enhancement and friction

factor in cylindrical blade type tube inserts. In the study, experimentally and numerically obtained Nusselt and friction factor values had a good agreement in comparison with the correlations provided in the literature. Obtained results from all tube inserts were compared to plain tube and it was determined that Nusselt number shows a clear increase in the presence of used turbulators. Tube inserts with short blades spacing demonstrated maximum Nusselt value in all Reynolds numbers. Ranking in terms of Nusselt values was as follow respectively:

$$Sy(10) > Sy(5) > Sy(3)$$

By using mean value in chosen Re numbers, maximum Nusselt was obtained at $Sy_1 = 101$ mm which was 24% more than that of plain tube and also it was 18.7 and 8.3% for $Sy_2 = 216$ and $Sy_3 = 340$ mm respectively. It was observed that both Nusselt number and friction factor increase with reduction of effective diameter. Obtained friction factor for three different blade distances, were compared to smooth tube which showed a certain

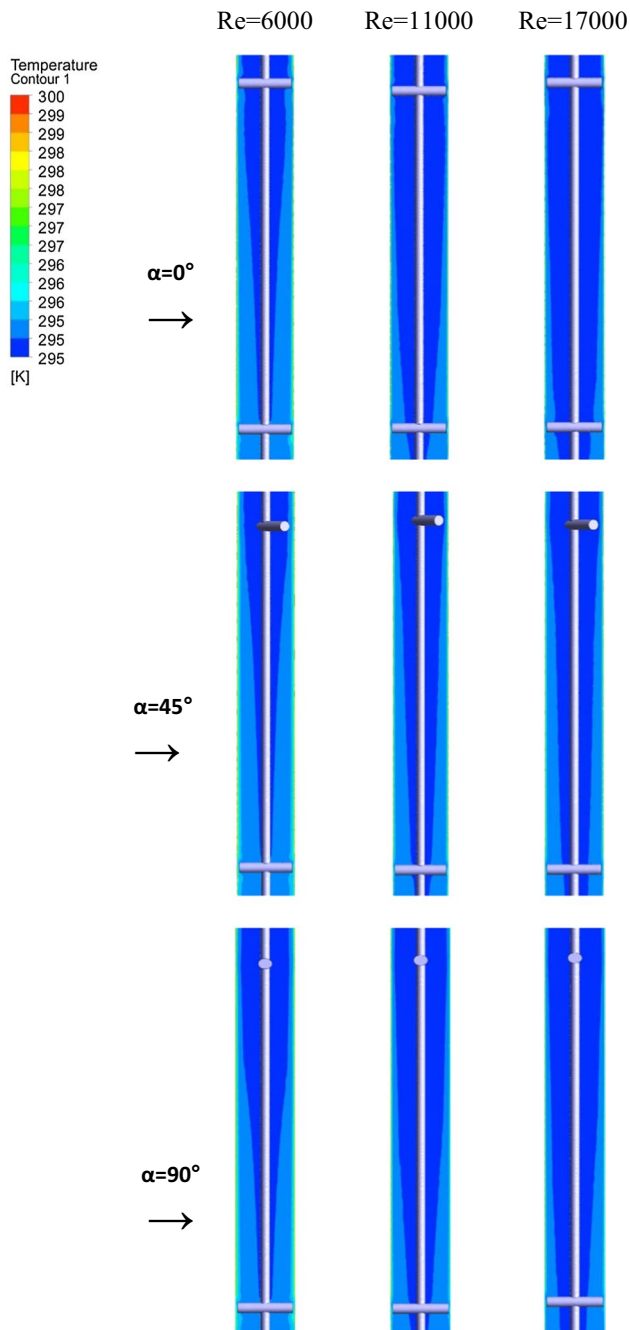


Fig. 23 Temperature contours for different Reynolds numbers at various angles

increase in the friction factor due to the used tube inserts. Turbulators with various blade angles were experimented in the test tube. It was determined that Nusselt number and friction factor don't show considerable change due to change in blade angle and the results were approximately identical. By simulation and visualization technique, heat flux and flow characteristics were observed along the length of the tube between blades and more detailed information about the tube inserts were obtained in this

way which is not experimentally available. The analysis method and CFD simulation applied in this study can be used to analyze other innovative types of tube inserts for evaluation heat transfer enhancement.

References

- Siddique M, Khaled A, Abdulhafiz N, Boukhary A (2010) Recent advances in heat transfer enhancements. *Int J Chem Eng Process* 106461:28
- Fan A, Deng J, Guo J, Liu W (2011) A numerical study on thermo-hydraulic characteristics of turbulent flow in a circular tube fitted with conical strip inserts. *Int J Appl Therm Eng* 31:2819–2828
- Eiamsa-Ard S, Thianpong C, Eiamsa-Ard P (2010) Turbulent heat transfer enhancement by counter/co-swirling flow in a tube fitted with twin twisted tapes. *Int J Exp Therm Fluid Sci* 34:53–62
- Jun-Dar C, Shou-Shing H (1991) Assessment study of longitudinal rectangular plate inserts as tube side heat transfer augmentative devices. *Int J Heat Mass Transf* 10:2545–2553
- Eiamsa-Ard S, Promvong P (2005) Enhancement of heat transfer in a tube with regularly-spaced helical tape swirl generators. *Int J Solar Energy* 78:483–494
- Eiamsa-Ard S, Thianpong C, Promvong P (2006) Experimental investigation of heat transfer and flow friction in a circular tube fitted with regularly spaced twisted tape elements. *Int Commun Heat Mass Transf* 33:1225–1233
- Chiu Y, Jang J (2009) 3D numerical and experimental analysis for thermal-hydraulic characteristics of air flow inside a circular tube with different tube inserts. *Int J Appl Therm Eng* 29:250–258
- Guo J, Fan A, Zhang X, Liu W (2011) A numerical study on heat transfer and friction factor characteristics of laminar flow in a circular tube fitted with center-cleared twisted tape. *Int J Therm Sci* 50:1263–1270
- Sivashanmugam P, Suresh S (2006) Experimental studies on heat transfer and friction factor characteristics of laminar flow through a circular tube fitted with helical screw-tape inserts. *Int J Appl Therm Eng* 26:1990–1997
- Yakut K, Sahin B (2004) The effects of vortex characteristics on performance of coiled wire turbulators used for heat transfer augmentation. *Int J Appl Therm Eng* 24:2427–2438
- Naphon P (2006) Heat transfer and pressure drop in the horizontal double pipes with and without twisted tape insert. *Int Commun Heat Mass Transf* 33:166–175
- Chang SW, Yang TL, Liou JS (2007) Heat transfer and pressure drop in tube with broken twisted tape insert. *Int J Exp Therm Fluid Sci* 32:489–501
- Yakut K, Sahin B (2004) Flow-induced vibration analysis of conical rings used for heat transfer enhancement in heat. *Int J Appl Energy* 78:273–288
- Promvong P, Eiamsa-Ard S (2007) Heat transfer augmentation in a circular tube using V-nozzle turbulator inserts and snail entry. *Int J Exp Therm Fluid Sci* 32:332–340
- Ozceyhan V, Gunes S, Buyukalaca O, Altuntop N (2008) Heat transfer enhancement in a tube using circular cross sectional rings separated from wall. *Int J Appl Energy* 85:988–1001
- Karagöz Ş (2015) Investigation of thermal performances of “S-shaped” enhancement elements by response surface methodology. *Int J Heat Mass Transf* 51:251–263
- Karakaya H, Durmus A (2013) Heat transfer and exergy loss in conical spring turbulators. *Int J Heat Mass Transf* 60:756–762

18. Selvaraj P, Sarangan J, Suresh S (2013) CFD analysis on heat transfer and friction factor characteristics of a turbulent flow for internally grooved tubes. *Int J Therm Sci* 17:1125–1137
19. Rahimi M, Shabaniyan S, Alsairafi A (2009) Experimental and CFD studies on heat transfer and friction factor characteristics of a tube equipped with modified twisted tape inserts. *Int J Chem Eng Process* 48:762–770
20. Kline S, McClintock F (1953) Describing uncertainties in single-sample experiments. *Mech Eng* 75:2–3
21. Hsieh S, Liu M, Wu F (1998) Developing turbulent mixed convection in a horizontal circular tube with strip-type inserts. *Int J Heat Mass Transf* 41:1049–1063
22. ANSYS Workbench, Fluent software (version 16)
23. Celik IB (2004) Procedure for estimation and reporting of discretization error in CFD applications. *ASME J Fluids Eng* 1(06):2008